Light Energy Conversion with Chlorophyll Monolayer Electrodes. In Vitro Electrochemical Simulation of Photosynthetic Primary Processes

Tsutomu Miyasaka,* Tadashi Watanabe, Akira Fujishima, and Kenichi Honda

Contribution from the Department of Synthetic Chemistry, Faculty of Engineering, The University of Tokyo, Hongo, Bunkyo-ku, Tokyo 113, Japan. *Received March 24, 1978*

Abstract: The photoelectrochemical behavior of chlorophyll (Chl) *a* and *b* monolayers, deposited on SnO_2 optically transparent electrodes by means of the Langmuir-Blodgett technique, has been investigated. Photocurrents and photovoltages were always anodic and negative, respectively, corresponding to an electron injection from excited Chl molecules to the conduction band of SnO_2. Spectra of photocurrents and photovoltages coincided well with the absorption spectra of Chl monolayers at the SnO_2-solution interface. Effects of light intensity, electrode potential, redox agents added, and solution pH on the magnitude of the photocurrent were studied in detail. The quantum efficiency for photocurrent generation was measured with Chl *a*-stearic acid mixed monolayers, and a highest value of 12-16% was attained at the Chl *a*/stearic acid molar ratio of ca. 1.0. The usefulness of the present system for an in vitro simulation of photosynthetic primary processes is suggested.

Introduction

There has been much recent interest in photochemical and photoelectric investigation of chlorophyll (Chl) and related pigments, principally in connection with the mechanism of photosynthetic primary processes as well as light energy conversion. Excitation of Chl *a* contained in the two plant photosystems (PS's) leads to the pumping of an electron by at least 1.2 V[1] from a level of water oxidation ($E_0' = +0.81$ V vs. NHE at pH 7) to that of ferredoxin reduction ($E_0' = -0.43$ V).[2] It is known that hydrogen evolution is also possible in PS I through excitation of a specific state of Chl *a*, called P700. In this respect, we[3] previously pointed out a similarity between the photoelectrolysis of water at a TiO_2 semiconductor electrode[4] and the primary processes in photosynthesis.

In vitro photoelectrochemical behavior of Chl has been studied for the first time by Tributsch and Calvin[5] in 1971. Recently Albrecht and his co-workers[6] investigated the photoconductivity of electrodeposited Chl *a* layers under dry and wet conditions. Cathodic photocurrent at Chl *a* aggregate on a platinum electrode in an electrochemical cell was reported by Fong et al.,[7] and a photogalvanic cell using a Chl *a* layer as a membrane was studied by Katz et al.[8] These and another similar work[9] mostly employed microcrystalline or aggregated Chl layers, obtained by electrodeposition or solvent evaporation, as the photoreceptor.

From biological observations, however, it has been proposed that Chl molecules on grana thylakoid membranes assume a highly ordered state, through hydrophobic interaction between phytol chains and lipids or proteins, and the local concentration of porphyrin rings is relatively high (ca. 0.2 M).[10] Reaction center Chl molecules, particularly P700 in PS I, are supposed to have a specific structure due to a further participation of hydrogen bonding.[11-13]

The photoactivity of in vitro Chl layers having an ordered structure has been studied with two modes of arrangement. The first is the incorporation of Chl molecules into a small lipid bilayer, which is used as a membrane separating two electrolyte solutions.[14] Although such a system is closer to the biological one, an inherent high resistivity of the lipid membrane results in a relatively low photoconversion efficiency. Moreover, much skill is required to handle the minute (ca. 1 mm in diameter) and delicate membrane. Liposomes could also be obtained by this method, and photoredox reactions through the membrane have been studied.[15] Another mode is the deposition of ordered Chl molecules on solid substrates by means of the Langmuir-Blodgett technique.[16] Monolayers and multilayers of Chl obtained by this technique have been reported[17,18] and employed in the study of intermolecular energy transfer.[19] Photoconductivity measurements on Chl multilayers placed between two electrodes in dry systems have also been undertaken,[20] but the observed photoresponse was generally too small to permit the use of such a system as a model of photosynthesis. Villar[21] prepared Chl *a* multilayers on a metal substrate and measured photocurrents in an electrochemical cell using KCl-containing glycerol as the electrolyte solution. However, a photoelectrochemical study on a single Chl monolayer, the most primitive system, was not attempted. Our preliminary measurement showed that a Chl *a* monolayer on a platinum plate had a considerably low photoactivity. This might be due to a very efficient quenching of the excited state of Chl by free electrons in the metal, as well as due to the reversibility of electron exchange between Chl* and the metal substrate.

These considerations have led us to use an optically transparent electrode (OTE) made of SnO_2, on which a single Chl monomolecular layer was deposited by the use of a Langmuir film balance with a rather simple procedure. SnO_2 is an electrode material well characterized[22,23] and has heretofore been employed in a number of photoelectrochemical investigations.[24-27] Electron injection from excited dyes to the conduction band of SnO_2 can take place with high efficiency,[25-27] and the backward electron flow is effectively prevented because of the rectifying property of the semiconductor-solution interface. Availability of large-area electrodes and a very high transparency in the visible region allow us a direct and precise measurement of the absorption spectrum of the deposited Chl monolayer, which is indispensable for the calculation of the quantum efficiency of photocurrent generation. Furthermore, the present system makes it easy to study the effects of Chl-Chl intermolecular distance as well as of coexisting substances upon the photoconversion efficiency, by diluting the monolayer with inert compounds and by adding various compounds in the electrolyte solution, respectively.

Experimental Section

Materials. Chlorophyll (Chl) *a* and *b* were prepared from fresh spinach leaves; first the crude extract of chloroplast in methanol was partially purified by repeated treatments with dioxane-water mixtures[28] and then the precipitated aggregates were isolated and subjected to a column chromatography on powdered sugar.[29] All solvents, dioxane, and sugar used were of reagent grade. Extraction and fragmentation were all carried out under dim green light. The peak positions and peak ratios in the absorption spectra of prepared Chl *a* and *b* in ether solutions fairly coincided with the reported val-

0002-7863/78/1500-6657$01.00/0

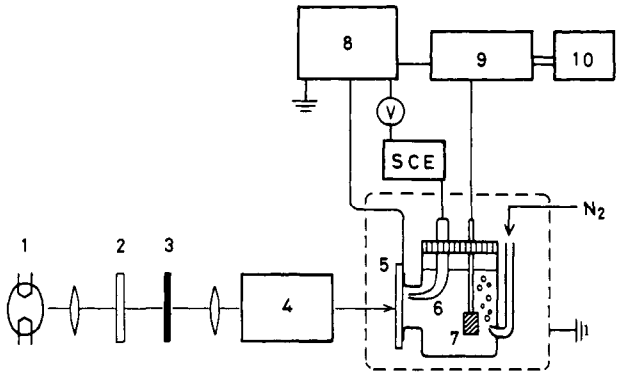

Figure 1. Schematic diagram of the photocurrent measurement: 1, light source; 2, filter; 3, shutter; 4, monochromator; 5, Chl-deposited SnO_2 OTE; 6, Luggin capillary; 7, Pt/Pt counterelectrode; 8, potentiostat; 9, picoammeter; 10, recorder.

ues.[17b,c,30] The purity of the sample was determined by means of empirical equations established by Comer and Zscheile.[31] The purified Chl samples were dissolved in distilled dry thiophene-free benzene at the concentration of 2×10^{-4} M after purging the solution with nitrogen, and stocked in the frozen state at −20 °C in darkness.

As the substrate for monolayer deposition, SnO_2 optically transparent electrode (OTE) (Matsuzaki Shinku Ltd.) was used. The electrode was 3 × 3 cm in size with one side being coated with SnO_2 layer 2000 Å thick. The SnO_2 layer had a specific resistance of 4×10^{-3} ohm·cm and an optical transmittance of 80–90% in the visible region above 400 nm. The donor density of the electrode was estimated to be ca. 10^{20} cm^{-3} from the slope of the Mott-Schottky plots.[32] Prior to the deposition of Chl monolayer, the electrode was washed repeatedly with hot organic solvents such as petroleum ether, acetone, and methanol, and was then treated with hot concentrated sulfuric acid and rinsed with water. The electrodes were preserved in a doubly distilled water before use. Sodium sulfate as an electrolyte, hydroquinone as a reducing agent, stearic acid as a diluent of Chl monolayer, and phosphate buffer solution were all reagent grade.

Monolayer Formation and Deposition. For the formation of Chl monolayers, a Langmuir trough (Kyowa Kagaku Ltd.) equipped with an Alexander-type surface balance[33] was employed. The inner walls as well as the edges of the trough (total volume 2.2 L, liquid surface area ca. 1000 cm^2) were coated with Teflon. The film balance consisted of a torsion wire and a thin mica floater, and could measure the surface pressure up to 40 dyn/cm with the accuracy of ±0.1 dyn/cm. The monolayer film was formed by delivering a 100–200 μl of 2×10^{-4} M Chl benzene solution onto the aqueous surface under dim green light. The surface pressure of monolayers was controlled by means of the Blodgett method[16a] or by slowly compressing the supernatant film with a Teflon barrier. Surface pressure-area isotherm (F-A curve) was measured at 25 °C for Chl *a* by compressing the film at the rate of 7–10 cm^2 min^{-1}.

The procedure of deposition of a monolayer onto the electrode surface was as follows. SnO_2 OTE was immersed vertically in the aqueous phase prior to spreading the Chl *a* benzene solution, and when the monolayer was formed to give a stable surface pressure, the OTE plate was lifted up at the rate of 3 cm min^{-1} by the use of a motor-driven elevator (Ishikawa Seisakusho Ltd.) under the constant surface pressure, 20 dyn/cm in most cases. The decrease in film area on the trough during the deposition was always recorded. All the procedures for monolayer formation and deposition were performed within 3 min under dim green light in order to avoid a possible slight degradation of the Chl film. Mixed monolayers of Chl *a* and stearic acid were formed and deposited on SnO_2 following the same procedures as above.

Absorption spectra of Chl *a* monolayers were measured on a Shimadzu spectrophotometer, Model MPS-5000, by stacking several electrodes in parallel, after washing off the Chl molecules on the glass side with acetone. Chl-free SnO_2 OTE's were used as reference. The precision of absorbance measurement was ca. ±0.0001 per layer. Absorptions of Chl monolayers at the SnO_2-electrolyte interface were also measured by immersing the Chl-deposited SnO_2 in a solution containing 0.1 M Na_2SO_4, 0.05 M hydroquinone, and 0.025 M pH 6.9 phosphate buffer.

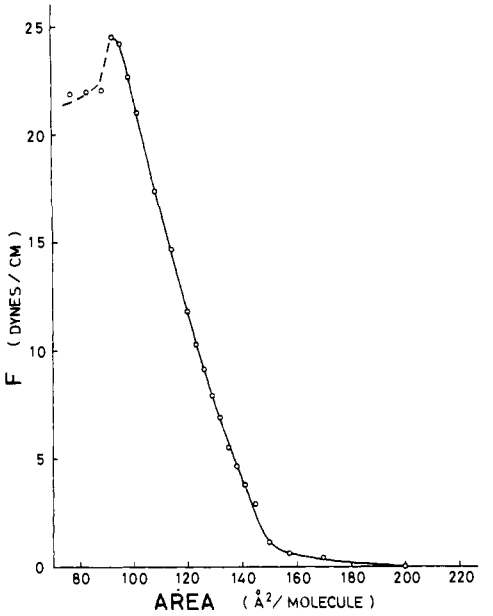

Figure 2. Surface pressure-area isotherm of Chl *a* monolayer: aqueous phase, 10^{-3} M phosphate buffer, pH 7.2; air atmosphere at 25 °C.

Photoelectrochemical Measurements. After a Chl-deposited SnO_2 OTE was dried, Chl molecules on the glass side was removed with acetone. To ensure an ohmic contact, a conductive silver paste was applied to one end of the SnO_2 surface and then connected with a lead wire. Figure 1 shows a schematic diagram of photoelectrochemical measurements. The electrode was mounted as a window of the electrochemical cell (volume 70 mL) to give ca. 4.9 cm^2 as the available area for electrolysis. The supporting electrolyte was 0.1 M Na_2SO_4 and during all experiments the solution was flushed with high purity nitrogen. The electrolyte solution contained, where necessary, hydroquinone and/or a suitable buffering agent. The potential of SnO_2 electrode was controlled by means of a Hokuto Denko potentiostat, Model HA-101, where a platinum wire and a saturated calomel electrode (SCE) served as the counterelectrode and the reference electrode, respectively. The electrochemical cell thus prepared as well as all the electrical cables were shielded with a common ground against electromagnetic perturbations.

As the light source, a 500-W xenon arc lamp (Ushio Electric Ltd. UXL-500D-O) was used in combination with a Shimadzu grating monochromator having a transmittance half-band width of ca. 10 nm and the spectral range 350–800 nm. For illumination experiments with wavelengths above 600 nm, a cut-off filter V-42 (Toshiba Kasei) was used. The number of photons incident to the electrode was determined by ferrioxalate actinometry at 390 nm[34] together with radiation energy measurements with a JASCO thermopile radiometer, Model RMA-8. Photocurrents were measured with a Keithley picoammeter, Model 417, and open circuit photovoltages were measured with a Keithley electrometer, Model 610 B. In the study of the effect of the pH value of the electrolyte solution on the photocurrent, a $NaOH-H_2SO_4$ system was employed.

Results and Discussion

Monolayer Properties. Figure 2 shows a typical surface pressure-area isotherm for Chl *a* on an aqueous phase (phosphate buffer, pH 7.2) at 25 °C. Under higher surface pressures of 24–25 dyn/cm, a sudden decrease in the pressure as reported by other workers[17b,c,35] was observed, and here the monolayer is considered to undergo a physical collapse. At surface pressures around 20 dyn/cm, where the area occupied by a Chl *a* molecule is about 100 $Å^2$, the film is expected to exist in the most packed state. In order to avoid a possible degradation of Chl under lower pressures on an aqueous phase,[35] all the experiments for monolayer deposition were performed under the surface pressure of 20 dyn/cm unless otherwise stated, and the time spent for deposition was minimized. During the deposition on SnO_2, the decrease in the surface area of the Chl film was

Table I. Properties of the Absorption Spectrum of Chlorophyll *a* Monolayer

	red peak		blue peak			surface pressure,
	λ, nm	O.D.	λ, nm	O.D.	blue/red[a]	dyn/cm
Trurnit and Colmano[17bb]	679	0.0094	423	0.0141	1.5	20
Bellamy et al.[17c]	680	0.011	440	0.013	1.18	15
Sperling and Ke[18a]	679	0.008	438	0.011	1.4	25
This work	676	0.0082	437	0.0103	1.25	20

[a] Absorbance ratio. [b] Values obtained by interpolation in the published data.

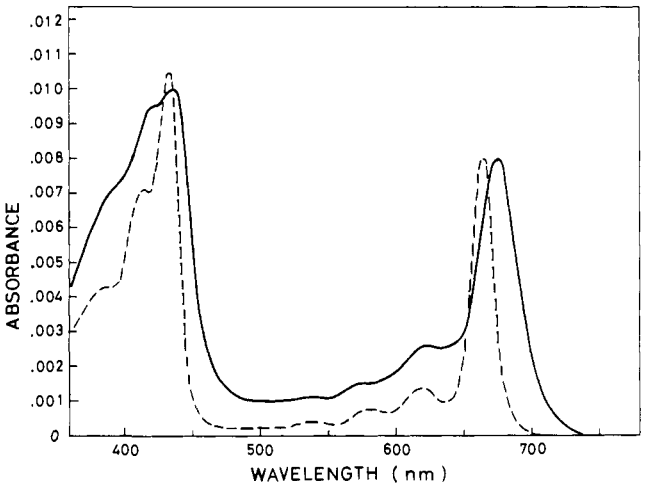

Figure 3. Absorption spectrum of Chl *a* monolayer at air-solid interface (solid curve). Dashed curve represents the absorption spectrum of a Chl *a* benzene solution (10^{-5} M) arbitrarily matched in scale at the red peak.

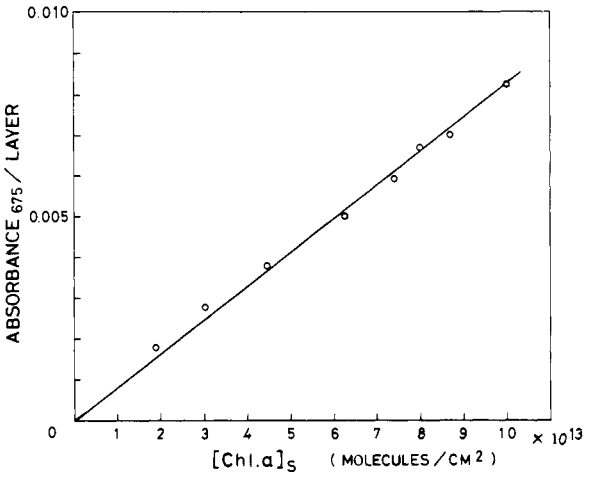

Figure 4. Relationship between the absorbance at 675 nm and the surface concentration of Chl *a* for Chl *a*-stearic acid mixed monolayers at air-solid interface.

always in fair agreement with the available surface area on the electrode.

On an aqueous surface, a Chl molecule is supposed to be oriented directing its porphyrin ring (ca. 15 Å in diameter) and the hydrophobic phytol chain (ca. 20 Å) upward and is anchored to water by the ester linkages in the molecule.[17c] Hence, in the course of upward lifting of a SnO_2 substrate, the Chl monolayer could be deposited with the hydrophilic ester linkages directed toward the SnO_2 surface, equally hydrophilic, with little change in the physical structure of the film. In fact, there occurred no deposition when a bare SnO_2 plate was immersed into the aqueous phase through the Chl film. Since the area of a porphyrin ring is ca. 200 $Å^2$, the value of 100 $Å^2$ occupied by a Chl molecule at 20 dyn/cm implies that under this condition the rings form a certain angle[36] against the aqueous as well as the substrate plane.

Absorption spectrum and absorbance of a Chl *a* monolayer deposited on SnO_2, measured at air-solid interface, agreed with those of a monolayer deposited on a microscope glass slide. Figure 3 compares the absorption spectrum of a Chl *a* monolayer with that of a Chl *a* benzene solution. Absorption maxima for the monolayer were found at 676 and 437 nm, with the absorbance of 0.0082 and 0.0103, respectively. Absorption data for the Chl *a* monolayer, together with the reported values,[17b,c,18a] are shown in Table I. In contrast to the case of an aggregated state, where an insertion of and subsequent adduct formation with foreign molecules like water could result in the generation of new absorption bands,[11-13] only slight bathochromic shifts by 10–15 nm are observed. This might be due to a highly packed structure of the present Chl *a* monolayer.

Upon immersion of a Chl *a* monolayer on SnO_2 into an electrolyte solution, there occurred some change in the spectroscopic properties. First the absorbance showed a decrease by 20–40% in both blue and red regions. But when the electrode was rinsed with water and dried, the reduced absorbance could be mostly recovered. Also a hypsochromic shift was observed in the red region from 676 nm in air to 671–672 nm in the electrolyte. In the blue region, a new peak appeared at 415 nm together with the original peak at 435 nm. Though the reason for such spectral changes upon immersion is not clear at the present stage, inorganic ions present at the SnO_2-solution interface might play some role in altering the polarization state of porphyrin rings.

For the purpose of controlling the surface concentration of Chl *a*, mixed monolayers of Chl *a* and stearic acid with various molar ratios were deposited on the electrode at 20 dyn/cm, and their absorption spectra were measured. Figure 4 shows the relationship between the absorbance at 675 nm and the surface concentration of Chl *a* in molecules cm^{-2} This result apparently suggests that the absorption coefficient in the red band undergoes little change by dilution. With increasing fraction of stearic acid, the blue absorption peak, 437 nm in a pure Chl *a* monolayer, showed a gradual shift to a limiting value of ca. 415 nm. This change was accompanied by a gradual increase in the absorbance ratio 415/675. Such a tendency might reflect a reaction of Chl *a* with surrounding acid leading to the formation of pheophytin,[37] as recently reported by Sperling and Ke.[18a] Upon immersion in an electrolyte solution, a spectroscopic change similar to the case of a simple Chl *a* monolayer was observed; the absorbance showed a general decrease, and a peak appeared at ca. 415 nm. Detailed spectroscopic data for Chl *a*-stearic acid mixed monolayers will be tabulated later in connection with the quantum efficiency measurements.

Photocurrent and Photovoltage Spectra. Owing to a large forbidden gap (3.7 eV[23]) and a small thickness (2000 Å), the background anodic photocurrent due to SnO_2 excitation was negligibly small in the visible region. This blank photocurrent had a measurable value at wavelengths below 400 nm, but did not exceed 2×10^{-8} A cm^{-2} even at 350 nm, the lower limit

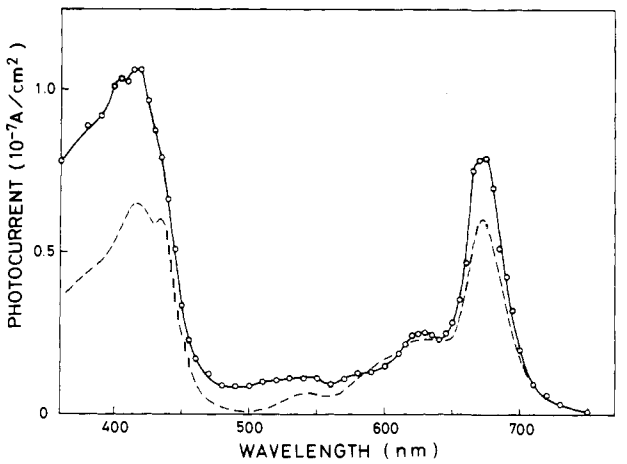

Figure 5. Photocurrent spectrum at Chl *a* monolayer on SnO_2 OTE: surface pressure of deposition, 20 dyn/cm; electrolyte composition, H_2Q 0.05 M, Na_2SO_4 0.05 M and phosphate buffer 0.025 M (pH 6.9); electrode potential, +0.05 V vs. SCE; incident monochromatic photon flux, 1.4×10^{15} cm^{-2} s^{-1}. The dashed curve represents the absorption spectrum of Chl *a* monolayer at SnO_2–electrolyte solution interface.

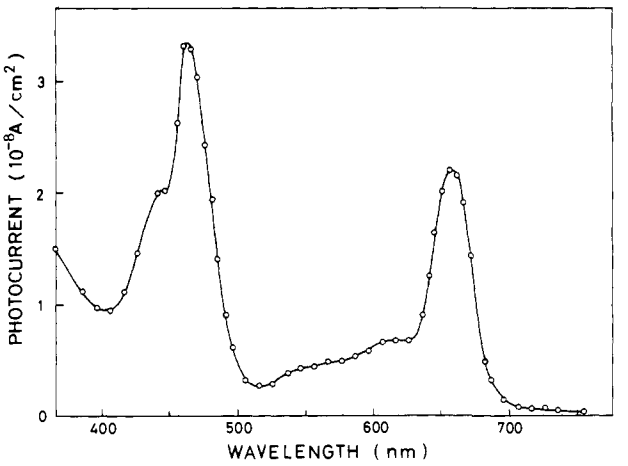

Figure 6. Photocurrent spectrum at Chl *b* monolayer on SnO_2 OTE: surface pressure of deposition, 10 dyn/cm; electrolyte composition, H_2Q 0.1 M and phosphate buffer 0.025 M (pH 6.9); electrode potential, +0.05 V vs. SCE.

in the present measurements. A correction for this blank photocurrent was performed where necessary.

At a SnO_2 electrode deposited with a Chl *a* monolayer, an anodic photocurrent was observed both under short-circuited condition and under potential-controlled condition in the range more anodic than −0.17 V vs. SCE. A typical photocurrent spectrum is illustrated in Figure 5 together with the absorption spectrum of a Chl *a* monolayer at SnO_2–solution interface. Photocurrents are corrected for the number of incident photons, based on the linear light intensity dependence described later, and correspond to the photon flux of 1.4×10^{15} photons cm^{-2} s^{-1}. As is evident in the figure, both spectra coincide fairly well showing the maxima at 420–415 and 675–672 nm. The blue/red peak ratio is ca. 1.4. This ratio tends to increase with increasing ionic strength in the electrolyte solution; e.g., it attains 1.6–1.8 in 0.1 M Na_2SO_4. This might suggest an influence of inorganic ions upon the electronic state and/or the molecular form of Chl *a* molecules at the SnO_2–solution interface, as mentioned above.

A similar photocurrent spectrum was obtained with a Chl *b*-deposited SnO_2 electrode, on which many fewer measurements were carried out in the present work, and an example is shown in Figure 6. Chl *b* monolayer was deposited on SnO_2

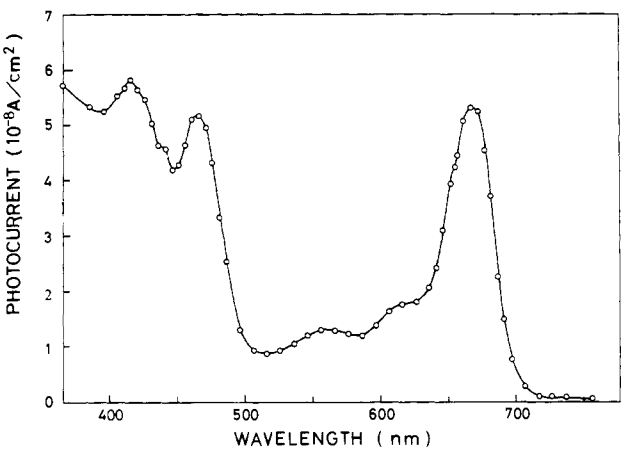

Figure 7. Photocurrent spectrum at Chl *a* + *b* (1/1) mixed monolayer: surface pressure of deposition, 15 dyn/cm; electrolyte and other conditions are the same as in Figure 6.

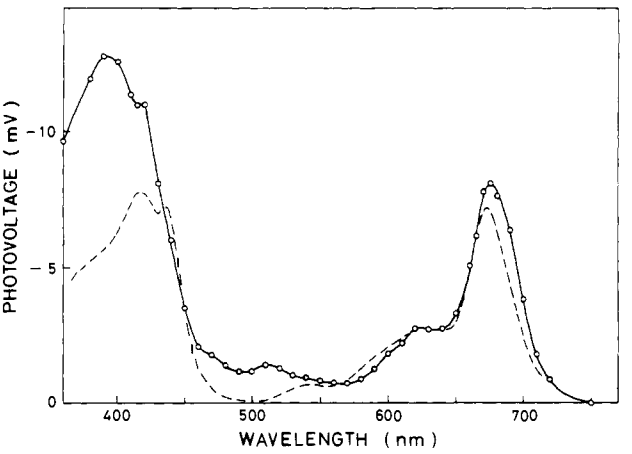

Figure 8. Open-circuit photovoltage spectrum at Chl *a* monolayer on SnO_2: surface pressure of deposition, 20 dyn/cm; electrolyte composition, H_2Q 0.05 M, Na_2SO_4 0.1 M, and phosphate buffer 0.025 M (pH 6.9); incident monochromatic photon flux, 1.4×10^{15} cm^{-2} s^{-1}. The dashed curve is the same as in Figure 5.

under a surface pressure of 10 dyn/cm. The peak wavelengths are situated at 463 and 657 nm, and the blue/red peak ratio is ca. 1.5. Since there exists some difference in photoactive wavelength regions for Chl *a* and *b*, an extention of spectral range is expected by using a monolayer containing both pigments. This is verified by Figure 7, which illustrates the photocurrent spectrum obtained with a SnO_2 electrode deposited with a monolayer consisting of Chl *a* and *b* to a molar ratio of 1.0.

An open circuit photovoltage was also measured monochromatically for Chl *a* monolayer, and an action spectrum is shown in Figure 8. In accordance with the generation of an anodic photocurrent (electron injection toward SnO_2), the observed photovoltage was always negative. The photovoltage spectrum also agreed well with the absorption spectrum at the SnO_2–solution interface, and the maximal values of 8 and 13 mV were obtained in the red and blue region, respectively.

Effect of Light Intensity. Dependences of the magnitude of Chl *a* photocurrent on the incident light intensity were measured at 675 and 415 nm, and the result is shown in Figure 9. The result is supposed to indicate that the primary stage of electron injection from excited Chl *a* to SnO_2 obeys a simple one-photon process,[38] at least up to the highest photon flux employed in the present study. Such a linear light flux dependence of anodic sensitized photocurrents has been reported with other dye–semiconductor combinations.[40]

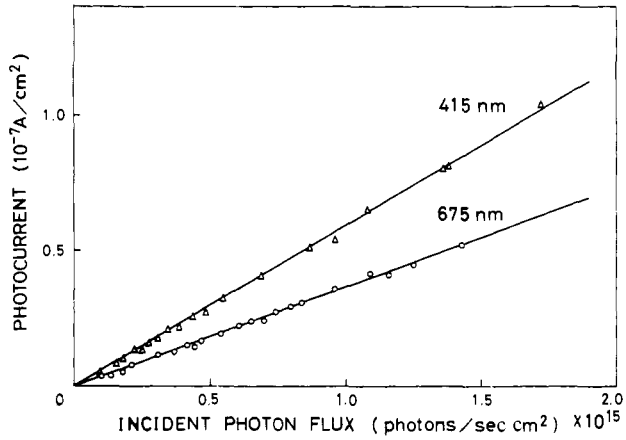

Figure 9. Dependence of Chl *a* photocurrent on the light intensity: electrode potential, −0.03 V vs. SCE. The electrolyte composition is the same as in Figure 8.

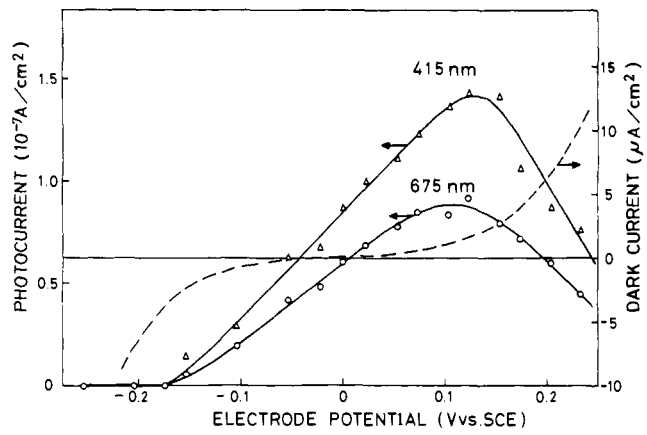

Figure 10. Photocurrent-potential curves at Chl *a* monolayer on SnO_2 OTE (solid curves). The electrolyte composition is the same as in Figure 8. Dashed curve represents the background dark current.

Effect of Electrode Potential. As already mentioned, the photocurrents observed by excitation of Chl monolayers on SnO_2 were anodic both under short-circuited and potential-controlled conditions, with essentially the same spectral responses. However, there appeared some difference in the time course of the photocurrent between the two cases. Under the short-circuited condition, the photocurrent showed a rapid rise upon the onset of illumination, followed by a slow decrease having a half-decay time of ca. 30 s. The final level of the photocurrent was ca. 70% of the initial value, and corresponded to about one-third of the maximal value under potential-controlled conditions. Turning off the light, the current rapidly decreased down to a cathodic value and then returned slowly to the zero level. Such a behavior has been reported for a Chl layer deposited on a platinum electrode.[7b,21] Under potentiostatic conditions, the decay characteristics were remarkably suppressed, and, in particular, almost no decay was observed in the presence of a reducing agent in the electrolyte solution. Because of the excellent reproducibility and stability of photocurrents, the present photoelectrochemical investigations were mostly carried out under potentiostatic conditions.

Figure 10 shows the potential dependence of photocurrents at Chl *a* deposited SnO_2 electrode in contact with an electrolyte solution at pH 6.9 containing hydroquinone as a reducing agent. The dark current is also illustrated in the figure. The anodic photocurrent due to Chl *a* excitation rises at −0.17 V vs. SCE and reaches a maximum at ca. +0.1 V. The photocurrent onset potential (−0.17 V) is somewhat more anodic than the flatband potential (−0.45 V vs. SCE[22]) of a SnO_2 electrode at pH 7. Such a result would reasonably be elucidated as follows. A simple calculation with the Mott-Schottky equation,[32] using the value of 10^{20} cm^{-3} as the donor density, gives the thickness of the space charge layer at the SnO_2 surface to be 17–27 Å in the potential range from −0.2 V to +0.2 V vs. SCE. Hence the space charge layer at potentials from −0.45 to −0.20 V is thin enough (less than 17 Å) to permit an efficient energy transfer from excited Chl molecules to the conduction electrons in SnO_2. This energy transfer could be followed by an energy dissipation as heat within the conduction band, and consequently the photocurrent becomes negligible in the region −0.45 to −0.17 V vs. SCE. A similar discussion has been presented by Pettinger et al.[41] concerning a rhodamine B sensitized photocurrent at a highly doped ZnO single crystal electrode. The decrease in the photocurrent at above +0.1 V vs. SCE corresponds to the increase in the dark current. This anodic dark current represents hydroquinone oxidation, and the photocurrent decrease may be due to the decrease in the effective hydroquinone concentration at the SnO_2–solution interface, as will be mentioned later.

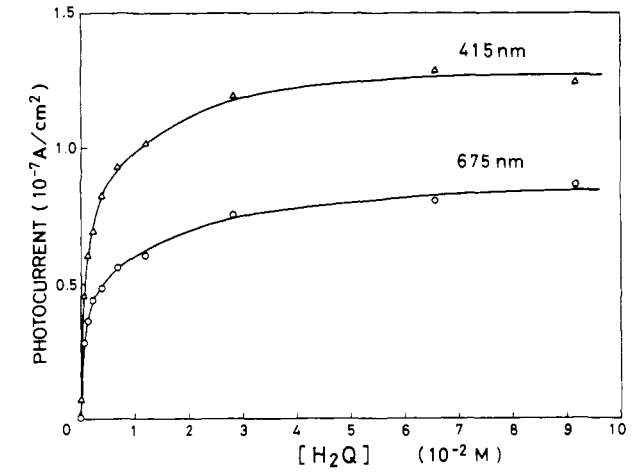

Figure 11. Dependence of Chl *a* photocurrent on H_2Q concentration: electrolyte, Na_2SO_4 0.1 M and phosphate buffer 0.025 M (pH 6.9); electrode potential, +0.1 V vs. SCE.

In the absence of hydroquinone, the photocurrent rises equally at ca. −0.17 V vs. SCE, and increases gradually with increasing anodic polarization until a maximal value is reached at about +0.7 V vs. SCE. The maximum photocurrent was ca. 0.7×10^{-8} A cm^{-2} by 675-nm illumination, and corresponded to ca. one-tenth of the maximum photocurrent observed in the presence of hydroquinone. Beyond +0.7 V, the photocurrent showed a decrease, due presumably to an electrochemical oxidation of ground-state Chl molecules.

Effects of Reducing and Oxidizing Agents. As described above, addition of hydroquinone (H_2Q) leads to an enhancement of the photocurrent due to excitation of Chl. Figure 11 shows the dependence of the photocurrent on H_2Q concentration, at +0.1 V vs. SCE and pH 6.9. The photocurrent increases with increasing H_2Q concentration and reaches a limiting value at $[H_2Q] \sim 5 \times 10^{-2}$ M. This limiting value is larger by a factor of 200–300 than the photocurrent in the absence of H_2Q at the same electrode potential. Hydroquinone possesses no optical absorption in the visible region. The observed photocurrent increase is considered to be essentially the same as the supersensitization[42,43] reported heretofore on other dye–semiconductor combinations. Two possible schemes have been proposed to account for the mechanism of supersensitization. One is the reduction of oxidized dye ($Chl^{+}\cdot$) resulting in the regeneration of photoactive state, and the other is the direct reduction of excited dye (Chl*) leading to the prevention of intramolecular recombination and/or of energy transfer to

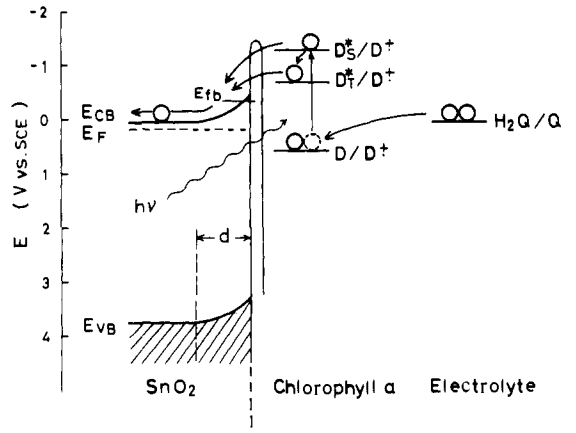

Figure 12. Schematic diagram for the electron transfer at Chl *a* monolayer on SnO_2. E_{CB}, E_{VB}, E_F, and E_{fb} denote the potentials (V vs. SCE) of the conduction band, valence band, Fermi level, and flatband of SnO_2, respectively. Redox potential for H_2Q/Q is shown on the right.

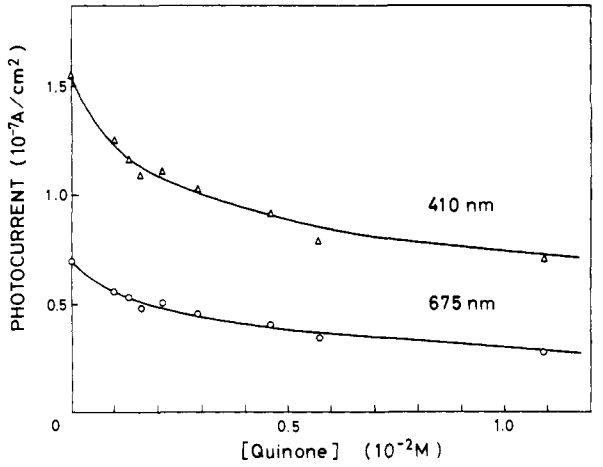

Figure 13. Dependence of Chl *a* photocurrent on *p*-quinone concentration: electrode potential, +0.1 V vs. SCE. The electrolyte composition is the same as in Figure 8.

the conduction electrons. Ascorbic acid also showed a similar supersensitizing effect in the present system. In this case, the photocurrent had a maximum at +0.15 V vs. SCE and the maximum value was comparable to that observed with H_2Q as a reducing agent.

A schematic diagram for electron transfer processes at a Chl *a* deposited SnO_2 electrode is illustrated in Figure 12. The values of pH and the electrode potential are tentatively assumed to be 7.0 and +0.1 V vs. SCE, respectively. At this pH, the flatband potential of SnO_2 is situated at −0.45 V vs. SCE,[22] and hence the potential drop within the space charge layer amounts to 0.55 V. Using the Mott–Schottky equation, the thickness, *d*, of the space charge layer at 0.1 V is calculated to give ca. 25 Å. Knowing the Chl *a* oxidation redox potential of +0.59 V vs. SCE[44] and the singlet and triplet excitation energies of 1.86 eV[45] and 1.26 eV,[46] one obtains the oxidation redox potentials for excited singlet and triplet states of Chl *a* as −1.27 and −0.67 V vs. SCE, respectively. Since these two levels are energetically higher than the conduction band edge of SnO_2, the electron-transfer paths as depicted in the figure are considered possible. In the absence of a reducing agent, the photocurrent remains small owing to the back transfer of an injected electron and/or an energy transfer followed by quenching, via the thin space charge layer. The coexistence of a reducing agent coud facilitate the unidirectional electron injection by the mechanism mentioned above.

On the other hand, addition of an oxidizing agent tends to decrease the photocurrent. Figure 13 shows the effect of *p*-quinone on the magnitude of the photocurrent, with the fixed H_2Q concentration of 5×10^{-2} M. Concerning the mode of action of an oxidizing agent, two schemes are considered possible: the extraction of a conduction electron injected from Chl* and the direct capture of an excited electron from Chl*. The decrease in the photocurrent, up to the *p*-quinone concentration of 10^{-2} M, is by a factor of 0.5 at most. Hence, the effect of *p*-quinone on the photocurrent is much smaller than that of H_2Q causing the photocurrent enhancement by a factor of 200–300. Therefore, the decrease in the photocurrent at potentials more anodic than +0.1 V vs. SCE (Figure 10) is supposed to result mainly from the electrochemical consumption of H_2Q in the interface region, rather than from the production of *p*-quinone. Even with an electrolyte solution containing only *p*-quinone as a redox agent, the Chl *a* photocurrent was always anodic at potentials above 0.0 V vs. SCE. This result indicates that the photooxidation of Chl *a* by *p*-quinone, if any, is a very ineffective pathway in the present photoelectrochemical system, and that there exists an efficient electronic coupling between the excited state of Chl *a* and the conduction band of SnO_2.

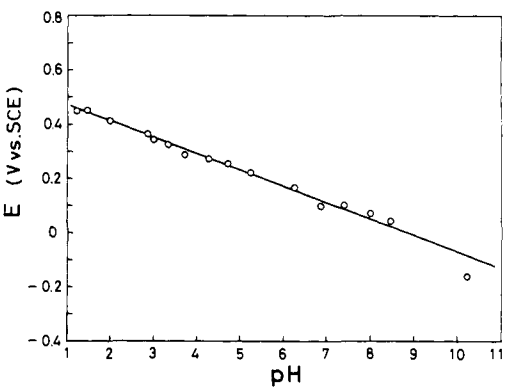

Figure 14. Dependence of the electrode potential generating the maximum photocurrent on pH of the electrolyte solution: electrolyte composition, H_2Q 0.05 M and Na_2SO_4 0.1 M. The straight line is drawn to indicate the slope of −60 mV/pH.

Effect of pH. In many instances, a change in pH of the electrolyte solution causes a shift of the semiconductor electrode potential (induced by a dissociation equilibrium of proton at the electrode surface) as well as of the equilibrium potential of a redox couple. In the present electrochemical system, not only the flatband potential of SnO_2[22] but also the oxidation redox potential of H_2Q can be shifted by ca. −60 mV per unit increase in the pH value. Therefore, the electrode potential corresponding to the maximum photocurrent (Figure 10) is expected to exhibit a cathodic shift with increasing pH. This prediction is verified by the experimental result illustrated in Figure 14.

It is also of interest to examine the influence of pH on the magnitude of the photocurrent due to Chl *a* excitation. Figure 15 shows the dependence of the maximum photocurrent by 675-nm excitation on the pH value, in the presence of H_2Q in the electrolyte solution. Apparently the photocurrent takes the largest value at pH around 4.0, and becomes smaller under both more acidic and more alkaline conditions. A similar behavior was observed also for Chl *a*–stearic acid mixed monolayers. On one hand, a decrease in pH value is expected to cause a downward shift of the energy level of SnO_2 against the redox levels of Chl *a*. This generally leads to an increase in the electron transfer efficiency in the anodic direction and would explain the behavior of the photocurrent in the region pH > 4. Similar conclusions have so far been reported with other dye–semiconductor combinations.[40c,47] At pH values above

Table II. Photocurrent Quantum Yields and Photovoltages at Chlorophyll *a*-Stearic Acid (C_{18}) Mixed Monolayers on SnO_2 Electrode

molar ratio Chl *a*/C_{18}	surface concn, 10^{13} mol cm^{-2}	absorption properties[a] absorbance red max[b]	absorbance blue max	blue peak, nm	abs ratio, 415/675	quantum yield of photocurrent,[c] % pH 6.9 red	pH 6.9 blue	pH 4.0 red	pH 4.0 blue	photovoltage[d] red max	photovoltage[d] blue max
Chl *a*	10.0	0.0082	0.0103	437	1.13	2.7	4.0	4.3	6.4	−8	−11
4/1	8.7	0.0070	0.0090	435	1.24	2.6	3.4	4.2	5.4	−9	−14
2/1	8.0	0.0067	0.0086	435	1.22	5.6	7.3	9.0	11.7	−11	−16
1/1	7.4	0.0059	0.0080	435	1.29	7.6	9.8	12.2	15.7	−14	−18
1/2	6.3	0.0050	0.0076	425	1.44	5.2	6.4	8.3	10.2	−14	−17
1/4	4.4	0.0038	0.0060	420	1.51	5.2	8.8	8.3	14.1	−13	−16
1/9	3.0	0.0028	0.0049	415	1.75	4.3	4.9	6.9	7.8	−8	−11
1/19	1.9	0.0018	0.0027	415	1.50	2.9	4.7	4.1	6.6	−4	−5

[a] At air-solid interface; pressure of monolayer deposition, 20 dyn/cm. [b] At 673-675 nm. [c] At red (~675 nm) and blue (~415 nm) peaks of photocurrent; accuracy, ±10%. [d] At pH 6.9; number of incident photons, 1.4×10^{15} cm^{-2} s^{-1}

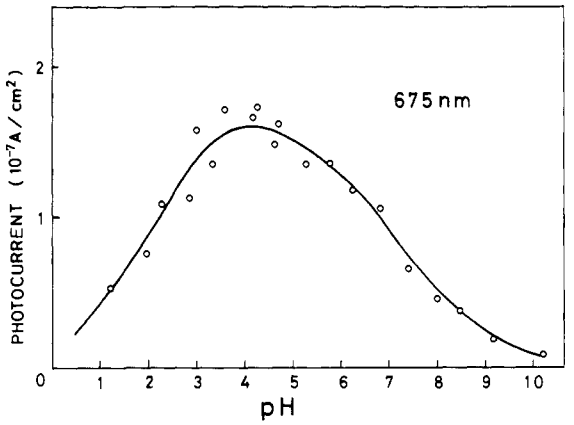

Figure 15. Dependence of the maximum Chl *a* photocurrent on pH of the electrolyte solution: electrolyte composition, H_2Q 0.05 M and Na_2SO_4 0.1 M. For each pH value, the electrode potential was adjusted to obtain a maximum photocurrent.

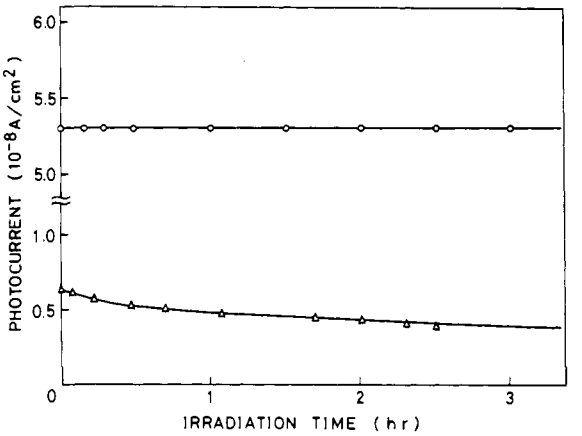

Figure 16. Time course of Chl *a* photocurrents (at 675 nm) in the presence and absence of hydroquinone: common electrolyte, Na_2SO_4 0.1 M and phosphate buffer 0.025 M (pH 6.9). —○—: with 0.05 M H_2Q; electrode potential, −0.02 V vs. SCE. —△—: without H_2Q; electrode potential, +0.6 V vs. SCE.

8, the shift in chemical equilibrium of H_2Q, leading to the formation of *p*-quinone, could be another cause for the photocurrent decrease. On the other hand, Chl *a* is known to undergo a decomposition resulting in the formation of pheophytin through the chemical reaction with proton.[48] We suppose, at the present stage, that such an instability of Chl *a* is mainly responsible for the decrease in the photocurrent in the acidic region.

Time Course of the Photocurrent. We measured the 675-nm photocurrents at a Chl *a* monolayer electrode as a function of illumination time, in the presence and absence of H_2Q in a neutral electrolyte solution. The result is shown in Figure 16. Here the electrode potential was chosen such that the dark current was negligibly small. When the electrolyte contained H_2Q, the photocurrent did not exhibit any decay characteristics for more than 7 h. This implies an excellent stability of the Chl *a* monolayer in spite of the continuous electron injection to SnO_2 from the excited state. In this case, apparently H_2Q is being oxidized quantitatively against the electric charge passing through the interface, as has been reported for other dye-semiconductor system.[49]

In the absence of H_2Q in the electrolyte solution, the photocurrent showed a decay by ca. 20% during the first 30 min. After that, the decay became much smaller. In this case, an oxidative decomposition of Chl *a*, following electron injection to SnO_2, may possibly occur during irradiation. If a one-electron process was assumed for this process, however, the total charge that has passed through the external circuit within the measurement period was apparently larger than that corresponding to the amount of Chl *a* molecules on SnO_2. Therefore, a trace amount of impurities having a reducing nature in the electrolyte must have acted in regenerating Chl *a* in the monolayer. Water itself could also be a candidate as an electron donor to the oxidized Chl *a*, as has been suggested by other workers.[7b,15b] However, further careful investigations will be necessary in order to finally sort out the principal reaction responsible for the sustained photocurrent flow in the absence of H_2Q.

Quantum Efficiency for Photocurrent Generation at Chl *a*-Stearic Acid Mixed Monolayers. Quantum efficiency for photocurrent generation at Chl *a*-stearic acid mixed monolayers, with various molar ratios, has been measured in electrolyte solutions at pH 6.9 and 4.0 containing 0.05 M H_2Q.[50] The quantum efficiency Φ_λ, at wavelength λ can be calculated by the following equation:

$$\Phi_\lambda = (I_{p\lambda}/q)/(F_{abs})_\lambda \quad (1)$$

where $I_{p\lambda}$ is the photocurrent (A cm^{-2}) at wavelength λ, q the elementary charge (coulombs), and $(F_{abs})_\lambda$ the number of photons (cm^{-2} s^{-1}) absorbed by the monolayer. $(F_{abs})_\lambda$ is calculated using the number of incident photons, $F_{i\lambda}$, and the absorbance, A_λ, of the monolayer in contact with the electrolyte solution, as follows:

$$(F_{abs})_\lambda = F_{i\lambda}(1 - 10^{-A_\lambda}) \quad (2)$$

Table II summarizes the results of photocurrent quantum efficiency and photovoltage measurements, together with the spectroscopic properties of Chl *a*-stearic acid mixed monolayers. For a Chl *a* simple monolayer in a neutral electrolyte, the value of Φ_λ was approximately 3 and 4% at the red and blue peak, respectively.[51] With increasing molar fraction of stearic

acid in the monolayer, both Φ_λ and photovoltage increase until maximal values are reached at the molar ratio Chl *a*/stearic acid = 1/1, and then tend to decrease at higher concentrations of stearic acid. The highest values of Φ_λ at Chl *a*/stearic acid = 1/1 and pH 4 are ca. 12 and 16% at the red and blue peak, respectively. These values are considerably larger than those reported as the photoconversion efficiency of Chl in other systems.[6,8,14b,15a] The increase of Φ_λ observed upon dilution of Chl *a* from 100% down to 50% is supposedly related to an increase in the Chl *a*–Chl *a* intermolecular distance (ca. 12 Å at Chl *a*/stearic acid = 1/1). A decrease in the intermolecular distance would lead to a decrease in the efficiency of Chl *a*–Chl *a* intermolecular energy transfer within the two-dimensional plane. An increase in fluorescence yield on lowering the Chl concentration in a mixed monolayer has been verified experimentally.[19] The occurrence of such an energy transfer, whose efficiency is necessarily less than unity, is expected to act in lowering the efficiency of electron injection to SnO_2. Memming[25] reported a similar result, i.e., a decrease in the photocurrent quantum efficiency with increasing surface concentration of a cyanine dye, from photoelectrochemical measurement.

Such a discussion appears to be inapplicable, however, to the *overall* photoconversion efficiency in photosynthetic systems in vivo. In this case, contrary to the present photoelectrochemical system, all the Chl molecules are not equivalent and an increase in the excitation energy transfer from antenna Chl molecules to the reaction center Chl is believed to enhance the overall efficiency.

As seen in the results in Table II, the value of Φ_λ decreases with decreasing surface concentration of Chl *a* beyond Chl *a*/stearic acid = 1/1. One of the possible causes for this phenomenon would be the chemical decomposition of Chl *a* yielding pheophytin,[48] as described above. A recent ESR study[52] showed that the triplet states of Chl and pheophytin are not very different from each other with respect to the photophysical behaviors. However, if one postulates that the observed photocurrent is caused by an electron injection from the singlet excited state of Chl *a* to SnO_2, a possibility remains that produced pheophytin brings about a lowering of Φ_λ. For a better understanding of this point, experiments should be carried out using a more inert compound (e.g., lipids) as a diluent for Chl *a* monolayer.

In conclusion, we could say that the present Chl monolayer/SnO_2 system constitutes, owing to its very high quantum efficiency for photocurrent generation, one of the most useful models for the photosynthetic primary processes. Our system can be regarded essentially as an in vitro electrochemical simulation of PS II, since the direction of the photocurrent is *anodic* and that the photoresponse red peak lies close to that of the in vivo reaction center P680. As mentioned above, a metal–Chl monolayer electrode seems inappropriate for PS II simulation, because of the possible effective quenching of the Chl excited state. The occurrence of an effective quenching implies the nonexistence of a process (supply of an electron by a donor to Chl*) fast enough to compete with quenching. If, on the other hand, there exists an *acceptor* which can extract an electron from Chl* with a rate greater than or comparable to that of quenching, a *cathodic* photocurrent would be generated with considerable efficiency. Such a case has been reported by Fong et al.[7] using Chl *a* hydrated polycrystals on Pt electrode. Their system can hence be regarded adequate for a simulation of system I rather than system II. For further experimental extention of these Chl electrodes, a combination of a Chl photocathode with photoanode would have much significance. Moreover, by utilizing the high transparency of the SnO_2 OTE, it would be possible to design an electrochemical photocell with high power conversion efficiency by alignment of many monolayer electrodes in parallel.

Acknowledgment. The authors are grateful to Mr. T. Inada for his assistance in part of the experiments. The present work was partially supported by a grant-in-aid from the Ministry of Education of Japan.

References and Notes

(1) Arnold estimated that, considering the necessity of redox overpotentials, the electron pumping could reach 2.3 V; cf. N. Arnold, *Proc. Natl. Acad. Sci. U.S.A.*, **73**, 4502 (1976).
(2) K. Tagawa and D. I. Arnon, *Nature (London)*, **195**, 537 (1962).
(3) A. Fujishima and K. Honda, *Bull. Chem. Soc. Jpn.*, **44**, 1148 (1971).
(4) A. Fujishima and K. Honda, *Nature (London)*, **238**, 37 (1972).
(5) H. Tributsch and M. Calvin, *Photochem. Photobiol.*, **14**, 95 (1971).
(6) (a) C. W. Tang, F. Douglas, and A. C. Albrecht, *J. Phys. Chem.*, **79**, 2723 (1975); (b) C. W. Tang and A. C. Albrecht, *J. Chem. Phys.*, **63**, 953 (1975); (c) C. W. Tang and A. C. Albrecht, *Nature (London)*, **254**, 507 (1975).
(7) (a) F. K. Fong and N. Winograd, *J. Am. Chem. Soc.*, **98**, 2287 (1976); (b) F. K. Fong, J. S. Polles, L. Galloway, and D. R. Fruge, *Ibid.*, **99**, 5802 (1977); (c) F. K. Fong and L. Galloway, *ibid.*, **100**, 3594 (1978).
(8) J. J. Katz, T. R. Janson, and M. R. Wasiliewski, *Proc. Karcher Symp. Energy Chem. Sci., Univ. Oklahoma*, 41 (May 1977).
(9) F. Takahashi and R. Kikuchi, *Biochim. Biophys. Acta*, **430**, 490 (1976).
(10) (a) F. Sjostrand, *Radiat. Res., Suppl. 2*, 349 (1960); (b) E. I. Rabinowitch, "Photosynthesis and Related Processes", Vol. 2, Interscience, New York, N.Y., 1956, p 1735.
(11) (a) L. L. Shipman, T. M. Cotton, J. R. Norris, and J. J. Katz, *Proc. Natl. Acad. Sci. U.S.A.*, **73**, 1791 (1976); (b) M. R. Wasiliewski, V. H. Smith, B. T. Cope, and J. J. Katz, *J. Am. Chem. Soc.*, **99**, 4172 (1977).
(12) S. G. Boxer and G. L. Closs, *J. Am. Chem. Soc.*, **98**, 5406 (1976).
(13) (a) F. K. Fong and V. J. Koester, *Biochim. Biophys. Acta*, **423**, 52 (1976); (b) F. K. Fong, A. J. Hoff, and F. A. Brinkman, *J. Am. Chem. Soc.*, **100**, 619 (1978); (c) L. Galloway, J. Roettger, D. R. Fruge, and F. K. Fong, *ibid.*, **100**, 4635 (1978).
(14) (a) W. T. Van and H. T. Tien, *J. Phys. Chem.*, **74**, 3559 (1970); (b) A. Ilani and D. S. Berns, *J. Membr. Biol.*, **8**, 333 (1972); (c) C.-H. Chen and D. S. Berns, *Photochem. Photobiol.*, **24**, 255 (1976).
(15) (a) M. Mangel, *Biochim. Biophys. Acta*, **430**, 459 (1976); (b) Y. Toyoshima, M. Morino, H. Motoki, and M. Sukigara, *Nature (London)*, **265**, 187 (1977).
(16) (a) K. B. Blodgett, *J. Am. Chem. Soc.*, **57**, 1007 (1935); (b) I. Langmuir and V. J. Shaefer, *ibid.*, **59**, 2075 (1937).
(17) (a) E. E. Jacobs, A. E. Vatter, and A. S. Holt, *Arch. Biochem. Biophys.*, **53**, 228 (1954); (b) H. J. Trurnit and G. Colmano, *Biochim. Biophys. Acta*, **31**, 434 (1959); (c) W. D. Bellamy, G. L. Gains, and A. C. Tweet, *J. Chem. Phys.*, **39**, 2528 (1963).
(18) (a) W. Sperling and B. Ke, *Photochem. Photobiol.*, **5**, 857 (1966); (b) G. L. Gaines, "Insoluble Monolayers at the Liquid-Gas Interface", Interscience, New York, N.Y., 1966.
(19) A. G. Tweet, G. L. Gaines, and B. D. Bellamy, *J. Chem., Phys.*, **40**, 2596 (1964).
(20) (a) W. Arnold and H. K. Maclay, *Brookhaven Symp. Biol.*, 11, 1 (1958); (b) K. J. McCree, *Biochim. Biophys. Acta*, **102**, 90, 96 (1965).
(21) J.-G. Villar, *J. Bioenerg. Biomembr.*, **8**, 199 (1976).
(22) F. Möllers and R. Memming, *Ber. Bunsenges. Phys. Chem.*, **76**, 469, 475 (1975).
(23) Z. M. Jarzebski and J. P. Marton, *J. Electrochem. Soc.*, **123**, 333C (1976).
(24) Th. Kuwana and W. R. Heineman, *Acc. Chem. Res.*, **9**, 241 (1976).
(25) R. Memming, *Faraday Discuss. Chem. Soc.*, **58**, 261 (1974).
(26) H. Kim and H. A. Laitinen, *J. Electrochem. Soc.*, **122**, 53 (1975).
(27) M. Fujihira, N. Ohishi, and T. Osa, *Nature (London)*, **268**, 226 (1977).
(28) K. Iriyama, N. Ogura, and A. Takamiya, *J. Biochem.*, **76**, 901 (1974).
(29) H. J. Perkins and D. W. A. Roberts, *Biochim. Biophys. Acta*, **58**, 486 (1962).
(30) H. H. Strain, M. R. Thomas, and J. J. Katz, *Biochim. Biophys. Acta*, **75**, 306 (1963).
(31) C. L. Comer and F. P. Zscheile, *Plant Physiol.*, **17**, 198 (1942).
(32) H. Gerischer in "Physical Chemistry: An Advanced Treatise", Vol. IXA, H. Eyring et al., Ed., Academic Press, New York, N.Y. 1970, p 487.
(33) A. J. G. Allan and A. E. Alexander, *Trans. Faraday Soc.*, **50**, 863 (1954).
(34) C. G. Hatchard and C. A. Parker, *Proc. R. Soc. London, Ser. A*, **235**, 518 (1956).
(35) G. Colmano, *Biochim. Biophys. Acta*, **47**, 454 (1961).
(36) R. M. Leblanc, G. Galinier, A. Tessier, and L. Lemieux, *Can. J. Chem.*, **52**, 3723 (1974).
(37) An unequivocal verification of the pheophytinization by means of optical absorption measurements in the wavelength range around 500 nm was not successful because of the less pronounced feature of the characteristic absorption bands in the monolayer state as reported by Bellamy et al.[17c]
(38) For the one-photon photochemical conversion process of Chl, semilinear photon flux dependence has been observed by McBrady and Livingston[39] and Fong et al.[13c] In such cases, a rather complicated reaction sequence leading to the final product, e.g., $Chl^{+\cdot}$, is postulated and the observed quantity (concentration change or photocurrent) is proportional to the amount of the final product. However, in our case, it will be reasonable to assume that the anodic photocurrent is directly proportional to the amount of Chl* at the Interface, since there exists a sufficient electronic coupling (overlap of the electronic distribution functions) between the Chl excited level and the conduction band of SnO_2.
(39) J. J. McBrady and R. Livingston, *J. Phys. Colloid Chem.*, **52**, 662 (1948).
(40) (a) K. Hauffe and J. Range, *Z. Naturforsch., Teil B*, **23**, 736 (1968); (b) M. Matsumura, Y. Nomura, and H. Tsubomura, *Bull. Chem. Soc. Jpn.*, **50**, 2533

(1977); (c) W. D. K. Clark and N. Sutin, *J. Am. Chem. Soc.*, **99**, 4676 (1977).
(41) B. Pettinger, H.-R. Schoeppel, and H. Gerischer, *Ber. Bunsenges. Phys. Chem.*, **77**, 960 (1973).
(42) P. B. Gilman, Jr., *Photogr. Sci. Eng.*, **18**, 418 (1974).
(43) H. Tributsch and H. Gerischer, *Ber. Bunsenges. Phys. Chem.*, **73**, 251 (1969).
(44) T. Saji and A. J. Bard, *J. Am. Chem. Soc.*, **99**, 2235 (1977).
(45) G. R. Seely, in "The Chlorophylls", Academic Press, New York, N.Y., 1966, p 541.
(46) B. A. Kiselev, Yu. N. Kozlov, and V. B. Evstigneev, *Dokl. Akad. Nauk SSSR*, **226**, 210 (1976).
(47) (a) E. Daltrozzo and H. Tributsch, *Photogr. Sci. Eng.*, **19**, 308 (1975); (b) T. Watanabe, A. Fujishima, O. Tatsuoki, and K. Honda, *Bull. Chem. Soc. Jpn.*, **49**, 8 (1976).
(48) S. H. Schanderl, G. O. Chichester, and G. L. Marsh, *J. Org. Chem.*, **27**, 3865 (1962).
(49) T. Watanabe, A. Fujishima, and K. Honda, *Ber. Bunsenges. Phys. Chem.*, **79**, 1213 (1975).
(50) In the absence of H_2Q in the electrolyte solution, the quantum efficiency did not exceed ca. 0.3%.
(51) In the present investigation, the measured photocurrent quantum efficiency in the blue region was always larger than that in the red region. The reason for this result has not yet been clarified at the present stage.
(52) J. F. Kleibeuker and R. J. Platenkamp, *J. Am. Chem. Soc.*, **98**, 3674 (1976).

Photoisomerization of Bis(9-anthryl)methane and Other Linked Anthracenes. The Role of Excimers and Biradicals in Photodimerization[1]

William R. Bergmark,*[2a] Guilford Jones, II,*[2b] Thomas E. Reinhardt,[2b] and Arthur M. Halpern[2c]

Contribution from the Departments of Chemistry, Boston University, Boston, Massachusetts 02215, Ithaca College, Ithaca, New York 14850, and Northeastern University, Boston, Massachusetts 02115. *Received March 14, 1978*

Abstract: Fluorescence characteristics, including quantum yields and lifetimes, and quantum efficiencies for photoisomerization (**1** → **2**) for a series of anthracenes linked at the 9 position have been measured. Emission yields and lifetimes (ns) decrease for the series dianthryl carbonate ($\tau_f = 5$), dianthrylethanes ($\tau_f \sim 2$), dianthrylmethanes ($\tau_f \leq 1$). Reaction quantum yields are not so much a function of chromophore linkage but are responsive to the substitution pattern at 10,10′ positions. For dianthrylethanes but not for dianthrylmethanes, excimer emission is observed for sandwich dimers generated in glasses at low temperatures. High photoreactivity for proximal anthracenes is identified with intersecting plane as opposed to parallel plane (sandwich excimer) geometries. In accord with recent theory, biradicals are proposed as intermediates in photodimerization. Formation and partitioning of these species (**14**) respectively control excited singlet lifetimes and photodimerization quantum yields. Thermochemical and kinetics data for the thermal back reaction (**2** → **1**) are reported. The measurement and significance of latent heats of isomerization (photon energy storage) are discussed.

Anthracene dimerizations have a long and important history in photochemistry. Solid-state photodimerization is generally observed and routine photolysis of moderately concentrated solutions of anthracene and a host of its derivatives leads to photodimers with relatively high chemical and quantum efficiency.[3] Photodimerization of the parent system was first reported in 1866[4] and quantum yield data were available as early as 1925.[5] The mechanism of photodimerization has been examined extensively over the last 2 decades, including an impressive gathering of spectroscopic and other photophysical data.[6]

It is not so widely appreciated that dimerization of anthracenes is a photoreaction which reversibly stores a significant fraction of photon energy as chemical potential energy[7] (i.e., the thermal back reaction is exothermic; vide infra). Weigert was the first to note this feature of storage and conversion of radiant energy.[8] More recently, anthracene photodimerization has been considered prototypical of cyclic organic systems with some potential for reversible storage of solar energy.[9]

We were attracted by an energy storage feature of *linked* anthracenes, intramolecular photoaddition of which requires formation of a small ring (**1** → **2**, where X = one- or two-atom link). Increased bond angle strain in photoisomers was expected to significantly amplify photon energy fixation. Linked chromophores also provide the possibility of enhanced absorption at long wavelengths due to chromophore interaction. Thus, a study of linked systems in principle provides an assessment of the potential for driving increasingly endoergic reactions with photons of decreasing energy.

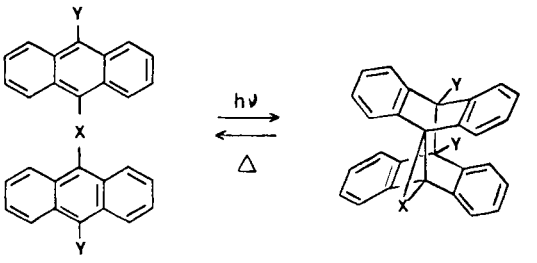

1 **2**

	X	Y
a	$-CH_2-$	H, H
b	$-CHOH-$	H, H
c	$-CHOH-$	H, OCH_3
d	$-CH_2CH_2-$	H, H
e	$-CH_2CH_2-$	CH_3, CH_3
f	$-OCO_2-$	H, H
g	$-CH_2CH_2-$	$-CH_2CH_2-$

The linked anthracenes were also expected to provide a test regarding intermediates in photodimerization. According to a widely held view of the mechanism,[6] excited singlet and

0002-7863/78/1500-6665$01.00/0